1 Draft Genome Sequence of *Lysinibacillus capsici* NAVL5D with Potential for Plant Growth Promotion

2 Mariska S. Kleyn[a], Muiz O. Akinyemi[a,b], Carlos Bezuidenhout[a], Rasheed A. Adeleke[a]

3 [a]Unit for Environmental Sciences and Management, North-West University, Potchefstroom, 2520,

4 South Africa.

5 [b]Leeds Institute of Health Sciences, University of Leeds, Leeds, LS2 9NL, United Kingdom

6 Corresponding author: rasheed.adeleke@nwu.ac.za

7

Abstract

The use of plant growth-promoting (PGP) bacteria is an emerging strategy for sustainable agriculture, offering alternatives to chemical fertilisers and pesticides. Here, we report the draft genome sequence of *Lysinibacillus capsici* NAVL5D which showed *in vitro* the potential to promote plant growth. This strain was isolated from the leaf of a lettuce plant grown in South Africa. The genome generated using the Illumina NovaSeq 6000 had a size of 4,631,824 bp, with 22 contigs and a G + C content of 37.3%. *In vitro* tests demonstrated the strain's potential for plant growth promotion through nitrogen fixation, phosphate solubilization, indole-3-acetic acid (IAA) production, hydrogen cyanide (HCN) synthesis, and siderophore production. Genome analysis revealed subsystems for auxin biosynthesis and nitrogen, phosphorus, and potassium metabolism, as well as PGP genes supporting these growth-promoting traits. Additionally, the genome predicted five biocontrol secondary metabolites, including terpenes and cyclic-lactone-autoinducers. However, eight pathogenicity-related genes and six antibiotic resistance genes were also identified, including *vanW*, *vanT*, *vanY*, *qacJ*, *msr(G)*, and *FosBx1*. Antibiotic susceptibility testing confirmed resistance to multiple antibiotics, particularly beta-lactams. Evidence of horizontal gene transfer was observed in the genome, which is significant given its established role in facilitating the spread of antibiotic resistance and virulence genes among bacteria. *In vivo* seed germination assays further demonstrated the strain's ability to promote plant growth, confirming its functional potential beyond in vitro observations. While *L. capsici* NAVL5D shows promise for sustainable agriculture applications, its potential pathogenicity and antibiotic resistance warrant further investigation to ensure its safe use as a plant growth-promoting agent.

Keywords: *Lysinibacillus capsici*, PGP, antibiotic resistant, endophyte, lettuce

30 Announcement

31 *Lysinibacillus*, a member of the Bacillaceae family, is a gram-positive, rod-shaped, endospore-forming
32 bacterium (Ahsan & Shimizu, 2021). *Lysinibacillus* strains have recently been explored for their diverse
33 ecological roles and potential attributes in plant growth promotion and biocontrol (Ahsan & Shimizu,
34 2021; Burkett-Cadena et al., 2019). *Lysinibacillus capsici,* in a symbiotic relationship with vegetables,
35 can enhance plant development through its versatile metabolic capabilities and resilience under harsh
36 environmental conditions (Kim et al., 2024). Strains of this bacterium have been reported as bio-
37 nutrient facilitators through the fixation of atmospheric nitrogen (Afzal et al., 2019; Kim et al., 2024),
38 and phosphate solubilisation (Kumar et al., 2025), making essential nutrients more accessible to plants
39 (Afzal et al., 2019; Kim et al., 2024)Click or tap here to enter text.. They are known to produce
40 various phytohormones, such as indole-3-acetic acid (IAA), a type of auxin that stimulates root growth
41 and enhance the plant's ability to absorb water and nutrients from the soil (Kurepin et al., 2014),
42 produce hydrogen cyanide (HCN), which at low concentrations, can act as a biocontrol agent against
43 plant pathogens (Sehrawat et al., 2022) Click or tap here to enter text.. Strains within this genus
44 are also known to produce siderophores, compounds that chelate iron from the environment, thereby
45 making the essential micronutrients available to plants and enhancing their metabolic functions and
46 stress resilience (Chaudhary & Sindhu, 2025). All these attributes, if harnessed effectively, can
47 potentially contribute to sustainable agriculture by reducing the need for agrochemicals. However, the
48 safety profile of endophytic bacteria should be carefully considered in the context of sustainable
49 agriculture. This study evaluated the PGP potential of *L. capsici* strain NAVL5D and characterized its
50 safety profile through integrated culture-dependent methods and whole-genome analysis.

51 *Lysinibacillus capsici* NAVL5D was isolated from the leaves of lettuce (*Lactuca sativa*) plants collected
52 from a smallholder farm in North-West Province, South Africa (26.6639° S, 25.2838° E). Healthy lettuce
53 leaf tissue samples were subjected to surface sterilisation using a combination of 85% ethanol and
54 2.5% sodium hypochlorite. Following surface sterilisation, the tissues were crushed, and one gram was

55 suspended in 19 mL nutrient broth and incubated at 37°C for 24 h. Pure isolates were obtained by
56 culturing 500 µL of the suspension on nutrient agar and sub-culturing three times on fresh nutrient
57 agar plates, incubated at 37°C for 24 h each time.
58 Genomic DNA was extracted from an individual pure colony of *L. capsici* NAVL5D using a Quick-DNA
59 Fungal/Bacterial Miniprep Kit from Zymo Research (Inqaba Biotec, South Africa). Library preparation
60 and pair-end sequencing (2 × 150 base pairs) were performed using the Illumina TruSeq Nano DNA
61 library preparation kit (Illumina) and the NovaSeq 6000 platform at the Novogene facility (Singapore,
62 Asia). The read quality of the sequence was determined using FastQC v0.12.0 (Andrews S, 2010).
63 Adapter trimming, quality filtering, and per-read quality pruning was performed using fastp v0.23.4
64 (Chen et al., 2018).
65 The sequence was assembled *de novo* into filtered paired-end reads using SPAdes v3.15.3 (Bankevich
66 et al., 2012). CheckM v1.2.2 (Parks et al., 2015) was used to evaluate genome completeness. The
67 assembly achieved a high coverage depth of 359.3 and was characterised as 99.34% complete with
68 1.21% contamination. The genome size for *L. capsici* NAVL5D was 4,631,824 bp, N50 was 2,566,169,
69 and GC content was 37.3%, with 22 contigs. Species designation of the strain was first determined by
70 extracting the 16S rRNA gene from the genome using extractseq version 5.0.0 (Rice et al., 2000) and
71 blasting against The National Center for Biotechnology Information 16S online database. Further
72 phylogenetic analysis identifying closely similar reference genomes and orthologous average
73 nucleotide identity (ANI) was performed using Mash v2.3 (Ondov et al., 2016). *L. capsici* NAVL5D had
74 98.91% ANI to *Lysinibacillus capsici* strain PB300 (ASM336750v1). Genome annotation was performed
75 using the Rastk (Brettin et al., 2015) and Prokka software (Seemann, 2014). Both annotations
76 predicted 4,690 protein-coding features and 76 non-coding features.
77 Prior to genome sequencing and annotation, the purified isolate was subjected to various qualitative
78 *in vitro* PGP tests performed in triplicates, while *Bacillus paralicheniformis* AJVR1 described by
79 Tsipinana *et al.* (2024) was used as positive control. The genetic determinant of the observed
80 phenotypes were thereafter identified.

The ability of *Lysinibacillus capsici* NAVL5D to fix nitrogen was tested by streaking a loopful of 24-h culture on Burk's nitrogen-free culture medium (HiMedia Laboratories, India) incubated for 7 days at 28°C (Orhan, 2016). Visible colony growth on nitrogen-free agar confirmed that *L. capsici* NAVL5D actively fixes atmospheric nitrogen (Figure 1a). Genomic analysis identified two *nif* genes (*nifS* and *nifU*) and an *iscS* paralog, all critical for synthesizing the nitrogenase enzyme complex. This enzyme catalyzes the conversion of atmospheric nitrogen (N_2) into ammonia (NH_3), a biologically accessible form of nitrogen. Additionally, genes encoding urease (*ureABC*) and its accessory proteins (*ureDEFG*) were detected. Urease hydrolyses urea into ammonia and carbon dioxide, while the accessory proteins activate the enzyme by inserting nickel into its inactive precursor. Though urease does not directly fix N_2, these genes enable the strain to recycle nitrogen from urea and maintain nitrogen balance during nitrogen fixation (Burén et al., 2020). This prevents ammonia toxicity by directing NH_3 toward biosynthesis, collectively explaining the observed nitrogen-fixing phenotype. Estimation of inorganic phosphate solubilisation was performed by spotting (about 3mm) fresh 24-hour culture of *L. capsici* NAVL5D on Pikovskaya medium (HiMedia Laboratories, India) as described by Kapadia et al. (2022). The 6.67 ± 0.58 diameter (mm) of clear halo around the pure colony (Figure 1b), indicates that *L. capsici* NAVL5D could solubilise phosphate. Genomic analysis indicates that *L. capsici* NAVL5D possesses 13 genetic elements collectively involved in phosphate acquisition, signalling, and metabolic adaptation. Central to this system is the pstSCAB-phoU operon , which encodes a high-affinity phosphate transport system critical for inorganic phosphate (Pi) uptake. This operon includes *pstS* (Pi-binding protein), *pstC* and *pstA* (membrane-spanning permease subunits), *pstB* (ATPase energy component), and *phoU* (negative regulator of Pi transport). (Baek & Lee, 2024). Additional genes, such as *ppk* and *ppk2* , encode polyphosphate kinases involved in polyphosphate storage and energy metabolism, and *phoH* contributes to phosphate homeostasis. The presence of *4-phytase* suggests capacity to hydrolyze phytate, releasing Pi for cellular use. Together, these genes coordinate nutrient scavenging, signaling, and metabolic flexibility, ensuring survival under fluctuating phosphate availability.

Indole-3-acetic acid (IAA) production by *L. capsici* NAVL5D was quantified using a colorimetric assay adapted from Lwin et al. (2012). The strain was cultured in nutrient broth supplemented with 5 µg/ml tryptophan at 35 °C for 5 days, followed by centrifugation at 3,000 rpm for 10 minutes to separate cellular biomass. The supernatant was reacted with orthophosphoric acid and Salkowski's reagent (50 ml 35% perchloric acid, 1 ml 0.5 M $FeCl_3$) under dark conditions for 30 minutes, generating a red complex proportional to IAA concentration. Absorbance at 530 nm, measured via spectrophotometry (Thermo Fisher Scientific, USA), yielded an average optical density value of 0.079 which was equivalent to 6.73 ± 0.346 µg/mL for *L. capsici* NAVL5D, confirming its IAA biosynthetic capacity relative to a pure IAA standard curve (Figure 1c). This phenotypic trait aligns with the presence of tryptophan biosynthesis genes (*trpA, trpB, trpC, trpD, trpE, trpG, trpS*), which encode enzymes critical for synthesizing tryptophan, a direct precursor for IAA production. While direct IAA-converting genes such as *iaaT, ipdC* were not identified in this analysis, the demonstrated IAA production suggests the presence of uncharacterized or alternative pathways for tryptophan-dependent IAA synthesis.

Hydrogen cyanide (HCN) production by *L. capsici* NAVL5D was assessed using the alkaline picric acid method (Castric & Castric, 1983; Reetha et al., 2014). Bacterial cultures were streaked onto nutrient agar plates supplemented with 4.4 g/L glycine (Sigma-Aldrich, USA). Sterile filter paper soaked in alkaline picric acid solution was affixed to the inner lid of each plate. Following sealing with Parafilm, plates were incubated at 30°C for 48 h alongside uninoculated control plates. A distinct colour transition of the filter paper from orange to brown confirmed HCN production by the strain (Figure 1d and e).

The observed HCN production reflects functional cyanogenesis supported by genomic determinants *rhodanese*, *sucC*, and *thiC*. While classic HCN biosynthesis is typically mediated by *hcnABC* genes (not detected here), the presence of *sucC* which encodes succinyl-CoA synthetase β-subunit indicates intact Tricarboxylic Acid cycle activity. This supplies ATP and carbon skeletons essential for glycine metabolism, where glycine serves as the direct precursor for HCN synthesis in non-canonical pathways. Concurrently, *thiC* enables biosynthesis of thiamine (vitamin B_1), a cofactor

132 required for glycine decarboxylase complexes that liberate HCN from glycine. Finally, *rhodanese*, a
133 cyanide detoxification enzyme converts toxic HCN into less harmful thiocyanate, allowing cellular
134 tolerance to self-produced cyanide. Together, these genes likely coordinate HCN synthesis, regulation,
135 and detoxification, ensuring the strain's ability to exploit cyanide-mediated mechanisms such as
136 inhibiting plant pathogens or competing with other microbes while mitigating self-harm.
137 The formation of an orange halo around *Lysinibacillus capsici* NAVL5D colonies on Chrome Azurol S
138 (CAS) agar (Sigma-Aldrich, USA) confirms active siderophore-mediated iron chelation. The assay was
139 conducted by incubating CAS plates inoculated with pure colonies for 3 days at 28°C (Kotasthane et
140 al., 2017). Genomic analysis revealed the presence of specialized iron acquisition systems. The
141 genes *cbrC* (a putative catechol siderophore regulator), *fhuF* (hydroxamate-type siderophore
142 receptor), *fhuD* (hydroxamate binding protein), *cbuB* (hydroxamate/carboxylate-type binding
143 protein), *fepC* (ABC transporter ATPase), and an Iron ABC transporter permease collectively enable
144 NAVL5D to efficiently scavenge iron, a nutrient critical for growth and survival in plants. In addition,
145 secondary metabolite of *L. capsici* NAVL5D were identified using the antiSMASH v.7.1.0 (Blin et al.,
146 2023). The strain was predicted to produce five biocontrol secondary metabolites, including terpenes
147 which contribute to both pathogen suppression and plant growth promotion and cyclic-lactone-
148 autoinducers which regulate behaviours like biofilm formation or antibiotic production.
149 To validate the plant growth-promoting potential of *L. capsici* NAVL5D, an *in vivo* seed germination
150 assay was conducted using lettuce (*Lactuca sativa*) seeds. The seedlings were coated with a bacterial
151 suspension standardised to 10^8 in 0.5% gum Arabic (Heidari Krush et al., 2025), while seeds coated
152 with bacteria free gum Arabic served as controls. Germination occurred in sterile water agar plates
153 cultivated in a climate-controlled growth chamber (Weiss Technik, Germany) at 25°C with 70%
154 relative humidity for 7 days (Figure 2). Ten biological replicates (five seeds/replicate) were established,
155 with growth parameters (seedling fresh weight, root length, coleoptile length, leaf length) quantified
156 via destructive sampling.

Data normality was verified using Shapiro-Wilk tests. Parametric data (equal variance confirmed by Brown-Forsythe test) were analysed using Welch's t-test; non-parametric data underwent Mann-Whitney Rank Sum tests to compare treatment versus control groups with significance thresholds set at $\alpha = 0.05$ for all treatment-control comparisons. *Lysinibacillus capsici* NAVL5D-inoculated seeds demonstrated significantly enhanced growth metrics relative to controls ($p < 0.05$), with morphological differences becoming evident within 72 hours of germination (Figure 3). By day 7, inoculated seedlings exhibited substantially increased biomass and organ development: mean fresh weight reached 8.5 ± 2.96 mg (vs. control: 6.07 ± 1.428 mg), while root elongation measured 11.7 ± 6.684 mm (vs. 4.6 ± 3.806 mm). Coleoptile and leaf dimensions similarly increased to 2.8 ± 1.317 mm and 3 ± 1.414 mm, respectively, significantly exceeding control measurements (Figure 3). Seedling growth quality was determined by calculating vigor index and germination rate (Walia et al., 2020).

$$Germination\ rate\ (\%) = \frac{Number\ of\ seeds\ germinated}{Total\ number\ of\ seeds\ sown} \times 100$$

$$Vigor\ Index = Germination\ Rate\ (\%) \times Seedling\ Length\ (cm)$$

Quantitative assessment of seedling performance revealed distinct responses to bacterial inoculation. While the control group achieved a marginally higher germination rate of 100%, *L.capsici* NAVL5D-treated seeds demonstrated a robust 90% germination success (Figure 4). More significantly, the vigor index showed dramatic enhancement in the treatment group, reaching 1,305 compared to the control value of 478. This 2.7-fold increase in vigor index highlights the strain's profound growth-promoting influence, where slightly reduced germination frequency is substantially compensated by superior seedling establishment and physiological robustness.

A multifaceted safety evaluation was conducted to assess potential consumer health risks associated with *L. capsici* NAVL5D, integrating phenotypic assays and genomic profiling. Virulence screening revealed three critical phenotypic indicators: γ-haemolysis (non-haemolytic) on sheep blood agar, confirming absence of cytolytic activity; protease production validated through casein hydrolysis; and

181 DNase negativity on Deoxyribonuclease Test agar, indicating limited nucleic acid degradation capacity.
182 These traits collectively suggest minimal virulence potential, as non-haemolytic activity eliminates
183 erythrocyte lysis concerns, protease function likely supports environmental adaptation rather than
184 pathogenicity, and DNase negativity reduces invasive potential. Genomic screening carried out by
185 querying the genome against the PHI-base v5.0 (Urban et al., 2022) database, using Abricate software
186 (Seemann, n.d.). identified eight putative virulence genes, including stress-response factors like *clpP*
187 (proteolytic complex) and *cspA* (cold shock protein), but no direct mammalian pathogenicity markers.

188 Antimicrobial susceptibility profiling via CLSI-standardized disk diffusion assay demonstrated
189 resistance to all tested β-lactams (Ampicillin, Penicillin G, Amoxicillin, Ceftriaxone, Cefixime, Ceftiofur),
190 Ciprofloxacin, Nitrofurantoin, and Trimethoprim when challenged with 22 antibiotics across nine
191 classes on Mueller-Hinton agar (Table 1; Supplementary figure 1) (Hudzicki, 2012; Weinstein & Lewis,
192 2020). Complementary genomic screening using Abricate identified detected six resistance
193 determinants on The Comprehensive Antibiotic Resistance Database (CARD v4.0.0) (Alcock et al.,
194 2023), including glycopeptide resistance genes (*vanW*, *vanT*, *vanY*), disinfectant resistance gene *qacJ*,
195 macrolide resistance gene *msr(G)*, and fosfomycin resistance gene *fosBx1*. These genotypic markers
196 correlate with observed phenotypic resistance to cell-wall inhibitors and 50S ribosomal subunit-
197 targeting antibiotics.

198 In conclusion, *L. capsici* NAVL5D exhibits robust plant growth-promoting capabilities, supported by a
199 combination of genomic and phenotypic traits that position it as a promising candidate for sustainable
200 agricultural applications. The strain's genetic arsenal includes key determinants for biocontrol, such as
201 genes involved in siderophore-mediated iron acquisition (*pchC*, *fepB*, *fhuF*), hydrogen cyanide
202 production (*rhodanese*, *thiC*), and secondary metabolite synthesis, which collectively enhance its
203 capacity to suppress phytopathogens. Additionally, its biofertilization potential is evident through
204 nitrogen fixation (*nifS*, *nifU*), phosphate solubilization (*pstSCAB-phoU operon*), and IAA biosynthesis
205 via tryptophan pathway genes (*trpA-E*, *trpG*, *trpS*). These multifaceted mechanisms align with

observed *in vivo* efficacy, where NAVL5D significantly improved lettuce seed germination rates, root elongation, and seedling vigor.

While these findings highlight NAVL5D's potential as a dual-function bioinoculant for enhancing crop productivity and reducing reliance on synthetic agrochemicals, rigorous further investigation is needed to address critical knowledge gaps. Specifically, long-term ecological studies are required to evaluate its environmental persistence, host-range specificity, and potential interactions with native microbial communities. Additionally, while phenotypic and genomic safety assessments revealed a non-hemolytic, DNase-negative profile with no overt mammalian virulence markers, comprehensive risk evaluations must extend to field-scale trials to ensure its deployment does not inadvertently disrupt agroecosystem balance or introduce unintended consequences for plant, animal, or human health.

Acknowledgement

This study was supported by the Water Research Commission of South Africa (project number C2022/2023-00962).

Author contribution

R.A.A: funding, conception, and study design; resources/reagents, manuscript editing. **M.S.K**: sample collection, preparation, experiments, first manuscript draft; **M.O.A**: sample collection, bioinformatic and data analyses, manuscript editing; **C.B**: critique, and manuscript editing.

Data availability

This Whole Genome Shotgun project has been deposited at DDBJ/ENA/GenBank under the accession number PRJNA1050647 and biosample SAMN38749212. The assembly reported here is ASM4015135v1

Declaration of interest

The authors declare that there are no conflicts of interest related to the financial or personal relationships that could influence the work reported in this article.

References

Afzal, I., Shinwari, Z. K., Sikandar, S., & Shahzad, S. (2019). Plant beneficial endophytic bacteria: Mechanisms, diversity, host range and genetic determinants. Microbiological Research, 221(December 2018), 36–49. https://doi.org/10.1016/j.micres.2019.02.001

Ahsan, N., & Shimizu, M. (2021). Lysinibacillus species: Their potential as effective bioremediation, biostimulant, and biocontrol agents. Reviews in Agricultural Science, 9(May), 103–116. https://doi.org/10.7831/ras.9.0_103

Alcock, B. P., Huynh, W., Chalil, R., Smith, K. W., Raphenya, A. R., Wlodarski, M. A., Edalatmand, A., Petkau, A., Syed, S. A., Tsang, K. K., Baker, S. J. C., Dave, M., Mccarthy, M. C., Mukiri, K. M., Nasir, J. A., Golbon, B., Imtiaz, H., Jiang, X., Kaur, K., … Mcarthur, A. G. (2023). CARD 2023: expanded curation, support for machine learning, and resistome prediction at the Comprehensive Antibiotic Resistance Database. Nucleic Acids Research, 51(1 D), D690–D699. https://doi.org/10.1093/nar/gkac920

Andrews S. (2010). FastQC: A Quality Control Tool for High Throughput Sequence.

Baek, S., & Lee, E. J. (2024). PhoU: a multifaceted regulator in microbial signaling and homeostasis. *Current Opinion in Microbiology*, *77*, 102401.

Bankevich, A., Nurk, S., Antipov, D., Gurevich, A. A., Dvorkin, M., Kulikov, A. S., Lesin, V. M., Nikolenko, S. I., Pham, S., Prjibelski, A. D., Pyshkin, A. V., Sirotkin, A. V., Vyahhi, N., Tesler, G., Alekseyev, M. A., & Pevzner, P. A. (2012). SPAdes: A new genome assembly algorithm and its applications to single-cell sequencing. Journal of Computational Biology, 19(5), 455–477. https://doi.org/10.1089/cmb.2012.0021

Blin, K., Shaw, S., Augustijn, H. E., Reitz, Z. L., Biermann, F., Alanjary, M., Fetter, A., Terlouw, B. R., Metcalf, W. W., Helfrich, E. J. N., Van Wezel, G. P., Medema, M. H., & Weber, T. (2023). AntiSMASH 7.0: New and improved predictions for detection, regulation, chemical structures and visualisation. Nucleic Acids Research, 51(W1), W46–W50. https://doi.org/10.1093/nar/gkad344

Brettin, T., Davis, J. J., Disz, T., Edwards, R. A., Gerdes, S., Olsen, G. J., ... & Xia, F. (2015). RASTtk: a modular and extensible implementation of the RAST algorithm for building custom annotation pipelines and annotating batches of genomes. *Scientific reports*, *5*(1), 8365.

Burén, S., Jiménez-Vicente, E., Echavarri-Erasun, C., & Rubio, L. M. (2020). Biosynthesis of nitrogenase cofactors. *Chemical Reviews*, *120*(12), 4921-4968.

Burkett-Cadena, M., Sastoque, L., Cadena, J., & Dunlap, C. A. (2019). Lysinibacillus capsici sp. nov, isolated from the rhizosphere of a pepper plant. Antonie van Leeuwenhoek, International Journal of General and Molecular Microbiology, 112(8), 1161–1167. https://doi.org/10.1007/s10482-019-01248-w

Castric, K. F., & Castric, P. A. (1983). Method for rapid detection of cyanogenic bacteria. Applied and Environmental Microbiology, 45(2), 701–702. https://doi.org/10.1128/aem.45.2.701-702.1983

Chaudhary, S., & Sindhu, S. S. (2025). Iron sensing, signalling and acquisition by microbes and plants under environmental stress: Use of iron-solubilizing bacteria in crop biofortification for sustainable

agriculture. Plant Science, 356(December 2024), 112496. https://doi.org/10.1016/j.plantsci.2025.112496

Chen, S., Zhou, Y., Chen, Y., & Gu, J. (2018). Fastp: An ultra-fast all-in-one FASTQ preprocessor. Bioinformatics, 34(17), i884–i890. https://doi.org/10.1093/bioinformatics/bty560

Heidari Krush, G., Rastegar, S., Ramezanian, A., & Hashemi, H. (2025). Innovative composite edible coatings of chia seed gum, gum Arabic incorporated with Nano-emulsion of Oliveria decumbens essential oil for prolonging navel orange fruit shelf life. International Journal of Biological Macromolecules, 307(P4), 142270. https://doi.org/10.1016/j.ijbiomac.2025.142270

Hudzicki, J. (2012). Kirby-Bauer Disk Diffusion Susceptibility Test Protocol Author Information. American Society For Microbiology, December 2009, 1–13.

Kapadia, C., Patel, N., Rana, A., Vaidya, H., Alfarraj, S., Ansari, M. J., Gafur, A., Poczai, P., & Sayyed, R. Z. (2022). Evaluation of Plant Growth-Promoting and Salinity Ameliorating Potential of Halophilic Bacteria Isolated From Saline Soil. Frontiers in Plant Science, 13(July), 1–14. https://doi.org/10.3389/fpls.2022.946217

Kim, T. J., Hwang, Y. J., Park, Y. J., Lee, J. S., Kim, J. K., & Lee, M. H. (2024). Metabolomics Reveals Lysinibacillus capsici TT41-Induced Metabolic Shifts Enhancing Drought Stress Tolerance in Kimchi Cabbage (Brassica rapa L. subsp. pekinensis). Metabolites, 14(2). https://doi.org/10.3390/metabo14020087

Kotasthane, A. S., Agrawal, T., Zaidi, N. W., & Singh, U. S. (2017). Identification of siderophore producing and cynogenic fluorescent Pseudomonas and a simple confrontation assay to identify potential bio-control agent for collar rot of chickpea. 3 Biotech, 7(2), 1–8. https://doi.org/10.1007/s13205-017-0761-2

Kumar, S., Diksha, Sindhu, S. S., & Kumar, R. (2025). Harnessing phosphate-solubilizing microorganisms for mitigation of nutritional and environmental stresses, and sustainable crop production. In Planta (Vol. 261, Issue 5). Springer Berlin Heidelberg. https://doi.org/10.1007/s00425-025-04669-2

Kurepin, L. V., Zaman, M., & Pharis, R. P. (2014). Phytohormonal basis for the plant growth promoting action of naturally occurring biostimulators. Journal of the Science of Food and Agriculture, 94(9), 1715–1722. https://doi.org/10.1002/jsfa.6545

Lwin, K. M., Myint, M. M., Tar, T., & Aung, W. Z. M. (2012). Isolation of plant hormone (Indole-3-Acetic Acid - IAA) producing rhizobacteria and study on their effects on maize seedling. Engineering Journal, 16(5), 137–144. https://doi.org/10.4186/ej.2012.16.5.137

Ondov, B. D., Treangen, T. J., Melsted, P., Mallonee, A. B., Bergman, N. H., Koren, S., & Phillippy, A. M. (2016). Mash: Fast genome and metagenome distance estimation using MinHash. Genome Biology, 17(1), 1–14. https://doi.org/10.1186/s13059-016-0997-x

Orhan, F. (2016). Alleviation of salt stress by halotolerant and halophilic plant growth-promoting bacteria in wheat (Triticum aestivum). Brazilian Journal of Microbiology, 47(3), 621–627. https://doi.org/10.1016/j.bjm.2016.04.001

Parks, D. H., Imelfort, M., Skennerton, C. T., Hugenholtz, P., & Tyson, G. W. (2015). CheckM: Assessing the quality of microbial genomes recovered from isolates, single cells, and metagenomes. Genome Research, 25(7), 1043–1055. https://doi.org/10.1101/gr.186072.114

Reetha, A. K., Pavani, S. L., & Mohan, S. (2014). ma'am notes HCN assay _ bacteria. 3(5), 172–178.

Rice, P., Longden, I., & Bleasby, A. (2000). EMBOSS: the European molecular biology open software suite. *Trends in genetics*, *16*(6), 276-277.

Seemann T. (n.d.). ABRicate, GitHub - tseemann/abricate: :mag_right: Mass screening of contigs for antimicrobial and virulence genes. Retrieved March 4, 2024, from https://github.com/tseemann/abricate

Seemann, T. (2014). Prokka: Rapid prokaryotic genome annotation. Bioinformatics, 30(14), 2068–2069. https://doi.org/10.1093/bioinformatics/btu153

Sehrawat, A., Sindhu, S. S., & Glick, B. R. (2022). Hydrogen cyanide production by soil bacteria: Biological control of pests and promotion of plant growth in sustainable agriculture. *Pedosphere*, *32*(1), 15-38.

Tsipinana, S., Obi, L., Amoo, S., & Adeleke, R. (2024). Plant growth-promoting potential of bacterial endophytes isolated from Lessertia frutescens. South African Journal of Botany, 174, 768–778. https://doi.org/10.1016/j.sajb.2024.09.043

Urban, M., Cuzick, A., Seager, J., Wood, V., Rutherford, K., Venkatesh, S. Y., Sahu, J., Vijaylakshmi Iyer, S., Khamari, L., De Silva, N., Martinez, M. C., Pedro, H., Yates, A. D., & Hammond-Kosack, K. E. (2022). PHI-base in 2022: A multi-species phenotype database for Pathogen-Host Interactions. Nucleic Acids Research, 50(D1), D837–D847. https://doi.org/10.1093/nar/gkab1037

Walia, M. K., Mohammed, Y. A., Franck, W. L., & Chen, C. (2020). Evaluation of early seedling development of Chickpea and its relation to seed yield. Agrosystems, Geosciences and Environment, 3(1), 1–9. https://doi.org/10.1002/agg2.20005

Weinstein, M. P., & Lewis, J. S. (2020). The clinical and laboratory standards institute subcommittee on Antimicrobial susceptibility testing: Background, organization, functions, and processes. In Journal of Clinical Microbiology (Vol. 58, Issue 3). https://doi.org/10.1128/JCM.01864-19

338 **Legends**

339 **Table 1**: Antimicrobial susceptibility profile of *Lysinibacillus capsici* NAVL5D determined using disk
340 diffusion method

341 **Table 2:** Plant Growth-Promoting Functional and Genomic Features of *Lysinibacillus capsici* NAVL5D

342 **Figure 1**: *In vitro* screening of *Lysinibacillus capsici* NAVL5D showing the following results: a) visible
343 growth suggesting a positive result for atmospheric nitrogen fixation; b) halo zones around triplicate
344 colonies indicating phosphate solubilisation; c) a control broth and a red coloration, denoting Indole-
345 3-acetic acid (IAA) production; d) uninoculated hydrogen cyanide plate; e) orange-brown colour
346 change representing a positive result for hydrogen cyanide production

347 **Figure 2:** Seed germination on water agar plates observed after 7 days: a) and b) control seeds; c)
348 and d) seeds treated with *Lysinibacillus capsici* NAVL5D

349 **Figure 3:** *In vivo* measurements of seed germination across 7 days, represented as bar graphs with
350 error bars and statistically significance indicated by p-values, comparing control seeds with
351 *Lysinibacillus capsici* NAVL5D treated seeds

352 **Figure 4:** Germination across 10 seed replicates: a) control group showing 100% germination; b)
353 *Lysinibacillus capsici* NAVL5D treated seeds showing 90% germination

354 **Supplementary figure 1:** Representative *In vitro* antibiotic susceptibility test for *Lysinibacillus capsici*
355 NAVL5D using disc diffusion method

356

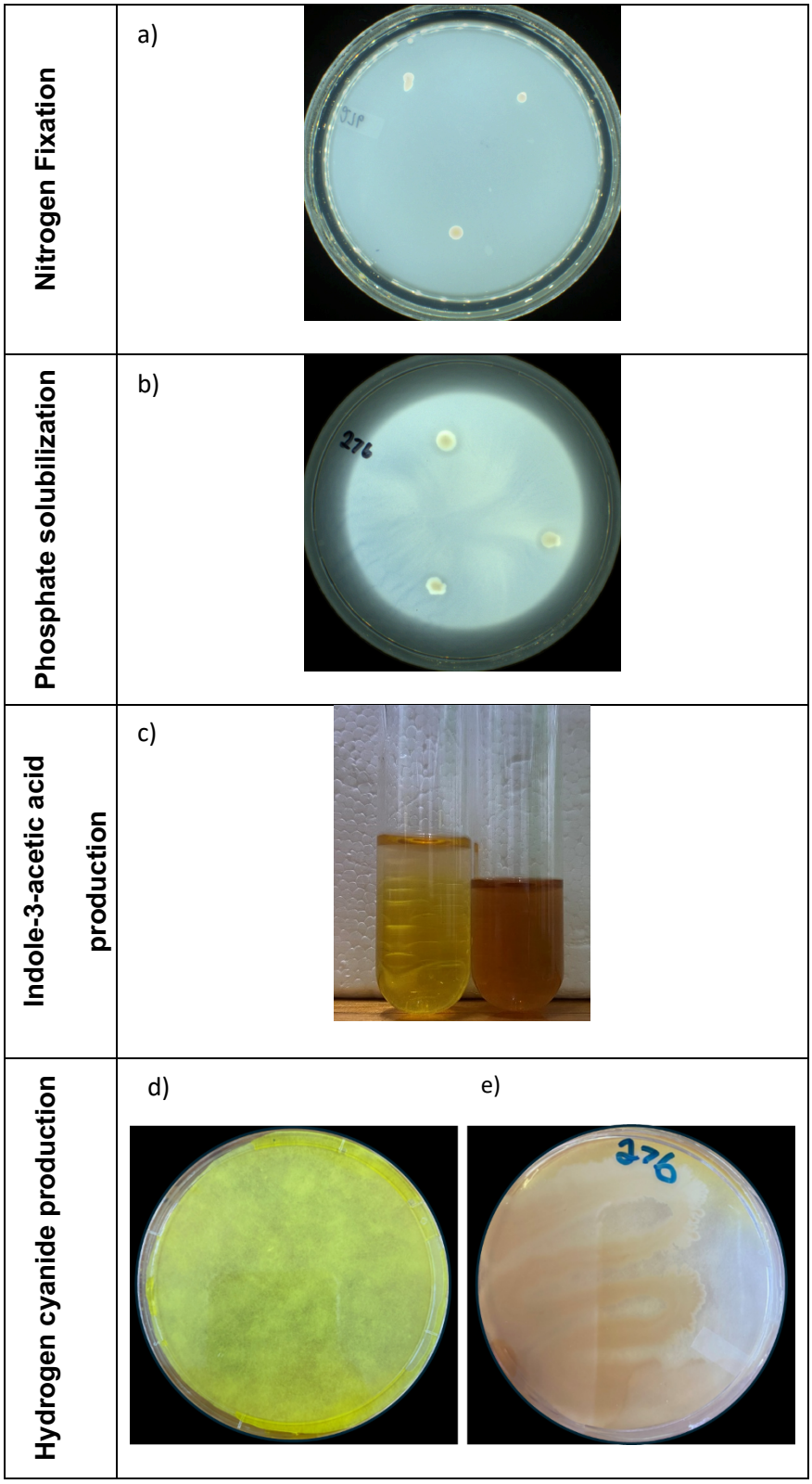

Figure 1: *In vitro* screening of *Lysinibacillus capsici* NAVL5D showing the following results: a) visible growth suggesting a positive result for atmospheric nitrogen fixation; b) halo zones around triplicate colonies indicating phosphate solubilisation; c) uninoculated hydrogen cyanide plate; d) orange-

brown colour change representing a positive result for hydrogen cyanide production; e) a control broth and a red coloration, denoting Indole-3-acetic acid (IAA) production

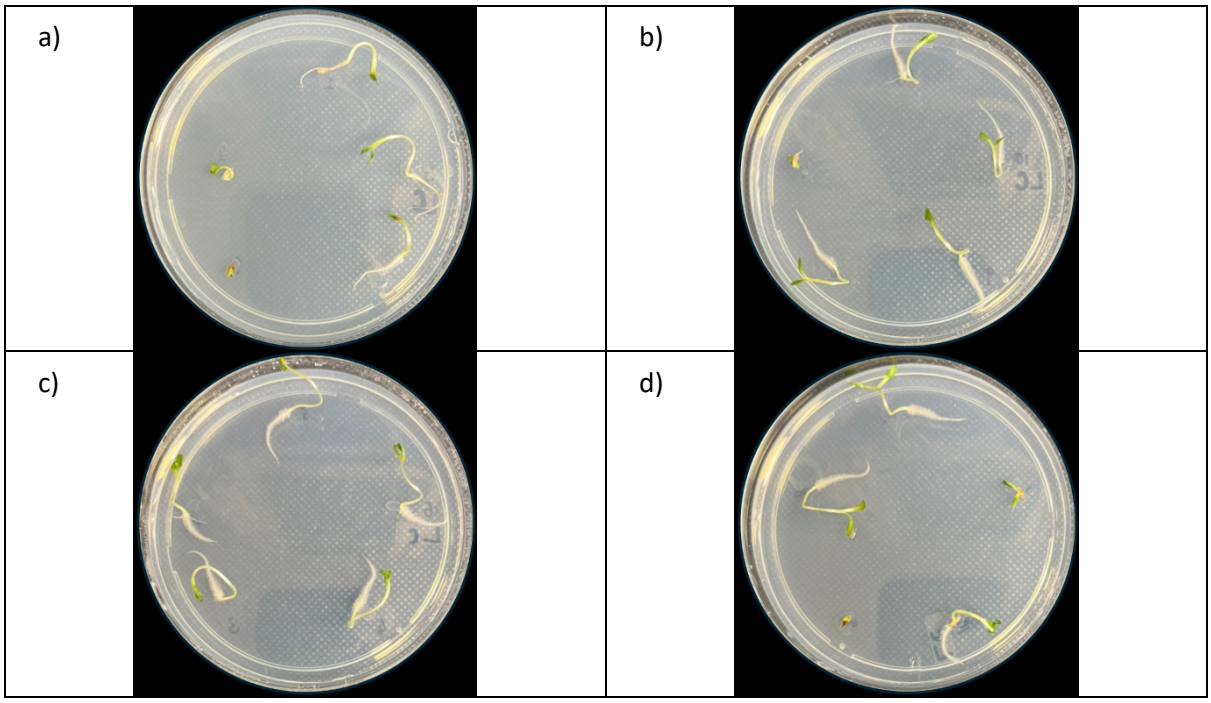

Figure 2: Seed germination on water agar plates observed after 7 days: a) and b) control seeds; c) and d) seeds treated with *Lysinibacillus capsici* NAVL5D

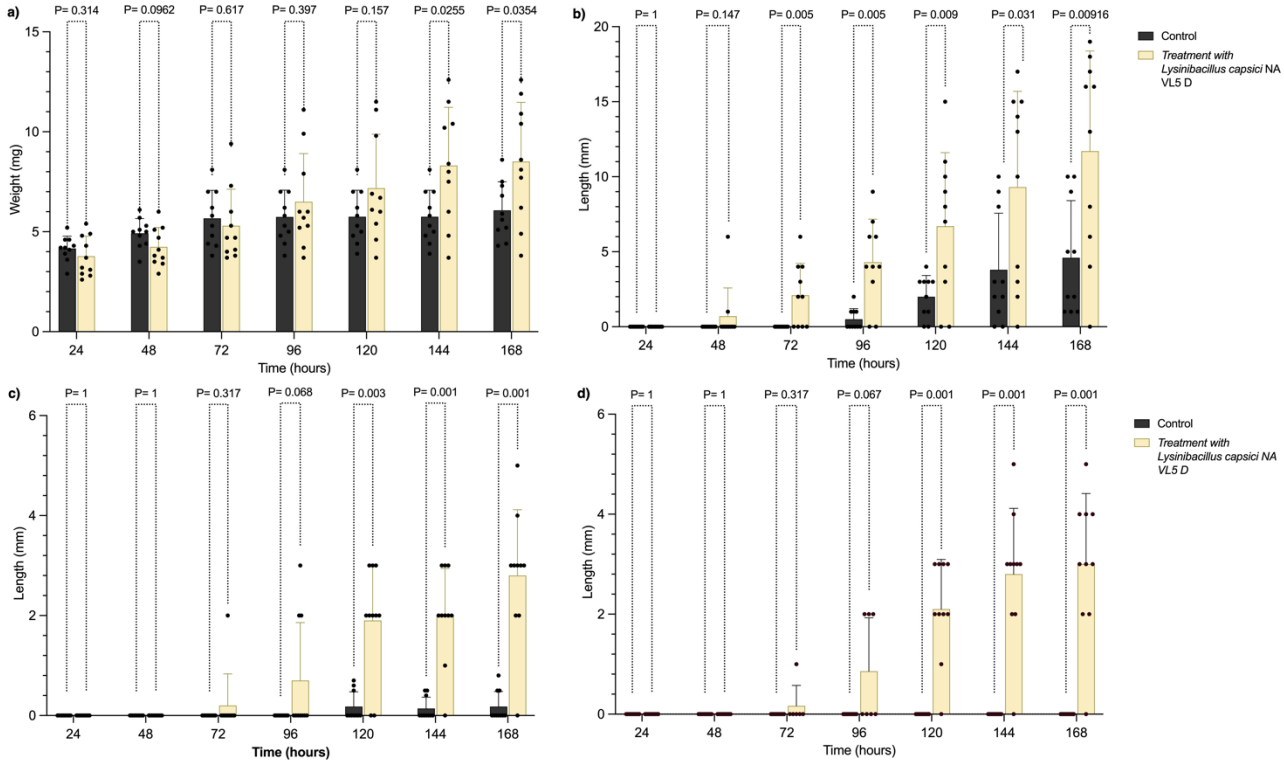

Figure 3: *In vivo* measurements of seed germination across 7 days, represented as bar graphs with error bars and statistically significance indicated by p-values, comparing control seeds with *Lysinibacillus capsici* NAVL5D treated seeds

Figure 4: Germination across 10 seed replicates: a) control group showing 100% germination; b) *Lysinibacillus capsici* NAVL5D treated seeds showing 90% germination

374 **Table 1**: Antimicrobial susceptibility profile of *Lysinibacillus capsici* NAVL5D determined using disk

375 diffusion method

Antibiotic (concentration)	Class	Mechanism of action	Phenotypic profile
Ampicillin (10 µg):	Beta-Lactam	Inhibition of Cell Wall Synthesis	Intermediate
Penicillin G (10 µg):	Beta-Lactam	Inhibition of Cell Wall Synthesis	Resistant
Amoxicillin (25 µg):	Beta-Lactam	Inhibition of Cell Wall Synthesis	Resistant
Ceftriaxone (30 µg):	Beta-Lactam	Inhibition of Cell Wall Synthesis	Resistant
Cefixime (5 µg):	Beta-Lactam	Inhibition of Cell Wall Synthesis	Resistant
Ceftiofur (30 µg):	Beta-Lactam	Inhibition of Cell Wall Synthesis	Intermediate
Doxycycline (30 µg)	Tetracyclines	30S Ribosomal Subunit Inhibitors	Susceptible
Oxytetracycline (30 µg)	Tetracyclines	30S Ribosomal Subunit Inhibitors	Susceptible
Tetracycline (30 µg)	Tetracyclines	30S Ribosomal Subunit Inhibitors	Susceptible
Clarithromycin (15 µg)	Macrolides	50S Ribosomal Subunit Inhibitors	Susceptible
Erythromycin (15 µg)	Macrolides	50S Ribosomal Subunit Inhibitors	Intermediate
Azithromycin (15 µg)	Macrolides	50S Ribosomal Subunit Inhibitors	Susceptible
Ciprofloxacin (5 µg)	Fluoroquinolones	DNA Gyrase and Topoisomerase IV Inhibitors	Resistant
Norfloxacin (10 µg)	Fluoroquinolones	DNA Gyrase and Topoisomerase IV Inhibitors	Susceptible
Levofloxacin (5 µg)	Fluoroquinolones	DNA Gyrase and Topoisomerase IV Inhibitors	Susceptible
Trimethoprim Sulfamethoxazole (25 µg)	Sulfonamides	Combination of Sulfonamide and Dihydrofolate Reductase Inhibitor	Susceptible

Trimethoprim (5 µg)	Sulfonamides	Dihydrofolate Reductase Inhibitors	Resistant
Clindamycin (2 µg)	Lincosamides	50S Ribosomal Subunit Inhibitors	Intermediate
Gentamicin (120 µg)	Aminoglycosides	30S Ribosomal Subunit Inhibitors	Susceptible
Streptomycin (300 µg)	Aminoglycosides	30S Ribosomal Subunit Inhibitors	Susceptible
Nitrofurantoin (300 µg)	Nitrofurantoin	Inhibition of Bacterial Enzyme Systems	Resistant
Chloramphenicol (30 µg)	Amphenicols	50S Ribosomal Subunit Inhibitors	Susceptible
Florfenicol (30 µg)	Amphenicols	Inhibition of Peptidyl Transferase Activity	Susceptible

Table 2: Plant Growth-Promoting Functional and Genomic Features of *Lysinibacillus capsici* NAVL5D

Functional trait	**Genetic related function**	***In vitro* Result**
Nitrogen fixation	*nifS, nifU, iscS, ureABC, ureDEFG*	Positive
Phosphate solubilisation	*pstA, pstB,, pstC, pstS, phoS, phoU, phoP, regX3, ppk, ppk2, phoH, phoR, 4-phytase*	Positive
IAA	*trpA, trpB, trpC, trpD, trpE, trpG, trpS*	Positive
HCN	*rhodanese, sucC, thiC*	Positive
Siderophores	*cbrC, fepC, fhuF, fhuD, Iron ABC transporter permease*	Positive

Supplementary figure 1: Representative *In vitro* antibiotic susceptibility test for *Lysinibacillus capsici* NAVL5D using disc diffusion method

381